EPR study of shallow and deep phosphorous centers in 6*H*-SiC

P. G. Baranov, I. V. Ilyin, and E. N. Mokhov
A. F. Ioffe Physico-Technical Institute, Polytechnicheskaya 26, 194021 St. Petersburg, Russia

H. J. von Bardeleben and J. L. Cantin
Groupe de Physique des Solides, Universités Paris 6&7, UMR 7588 au CNRS, 2 place Jussieu, 75005 Paris, France
(Received 17 January 2002; revised manuscript received 30 April 2002; published 7 October 2002;
publisher error corrected 14 October 2002)

The phosphorus related defects in *n*-type 6*H*-SiC monocrystals doped by neutron transmutation have been studied by electron paramagnetic resonance (EPR) spectroscopy. After thermal annealing at 1900 °C two sets of three phosphorous related EPR spectra are observed, which are attributed to the isolated shallow P donor on the two quasicubic ($c1$,$c2$) and the hexagonal (h) sites as well as to a deep P center on the $c1$, $c2$, h sites. The deep P center is tentatively attributed to the P_{Si}-carbon vacancy complex. Our results show in agreement with theoretical predictions that the previous suggestions that the two types of centers are the ground and excited states of the isolated P donor can be ruled out. The donor-monovacancy complexes are characterized by an exceptional thermal stability.

DOI: 10.1103/PhysRevB.66.165206 PACS number(s): 61.80.Hg, 76.30.Da, 61.72.Ji

INTRODUCTION

n-type conductivity of silicon carbide monocrystals is generally achieved by the use of nitrogen doping. The properties of the N donor in 6*H*-SiC have been studied in detail.[1,2] Nitrogen introduces shallow effective-mass-like donor states and is believed to substitute for carbon atoms. The properties of the isolated substitutional nitrogen donor depend further on the particular lattice site on which it is located. In the 6*H* polytype with three nonequivalent substitutional lattice sites, two quasicubic ($c1$,$c2$) sites and one hexagonal (h) site, three different N centers have been identified. Their thermal ionization energies are 81, 137.6, and 142.4 meV, respectively, with the hexagonal site donor being the shallowest one.

n-type conductivity can also be obtained by doping with phosphorous,[1,3–7] which can be introduced during the growth or after the growth; both ion implantation and neutron (n) transmutation have been used in the past. In the two cases, subsequent high-temperature thermal annealing is required to electrically activate the phosphorous dopant and to anneal the implantation related deep defects. In analogy to the case of shallow N, three different P centers corresponding to P on the $c1$, $c2$, h sites are expected to coexist. This picture is in agreement with electrical measurements on P-implanted, thermally annealed 6*H* layers.[6] They have shown the presence of two P related centers with ionization energies of (80 ± 5) and (110 ± 5) meV, which were attributed to the isolated P donor on the h site and the nondistinguished P donors on the $c1$ and $c2$ sites, respectively.

The microscopic and electronic structure of the phosphorous related defects can be studied in more detail by electron paramagnetic resonance (EPR) and electron-nuclear double resonance (ENDOR) spectroscopy. Such measurements have been performed only on neutron transmutation P doped *n*-type samples.[3–5] The results indicated a complex situation. Instead of the expected three P centers on the $c1$, $c2$, h sites, five different P related centers were observed in the 77–4.2 K temperature range. Their interpretation has given rise to some controversy, which is not yet settled. The first X-band EPR results were obtained by Veinger *et al.*[3] who observed at 77 K three different doublet spectra labeled $P1$, $P2$, P-V. They attributed the $P1$, $P2$ spectra to the isolated P_{Si} donor on the hexagonal and the nondistinguished $c1$, $c2$ sites; the third spectrum, P-V, was attributed to a different P related complex center. Kalabukhova, Lukin, and Mokhov[4] extended the EPR measurements to the 4 K temperature range and to higher frequencies (142 GHz). The sample investigated in their study had been *n*-irradiated under similar conditions as Veinger's sample but annealed at higher temperatures. They observed at 4 K two different P related centers—labeled $I1$, $I2$—with strongly reduced central hyperfine interactions (Table I); as these centers could only be observed at temperatures below 15 K, an inverted level system was proposed for the shallow P donor with an E ground state corresponding to the $I1$, $I2$ spectra and an A_1 excited donor state giving rise to spectra $P1$, $P2$, P-V.[1,5,8]

ENDOR measurements at 4.2 K confirmed[5] the phosphorous origin of the observed hyperfine splittings of the $I1$, $I2$ centers. It remained however unclear, why only two distinct sites were observed for this P center, whereas *a priori* three sites ($c1$,$c2$,h) are expected, and why the ground-state configuration should be different for shallow N and P donors.

The experimental results obtained up to 1997 for the N and P donors were resumed in Ref. 1. However, as shown in Table I the results contain some inconsistencies, which had not been noticed at that time. The numerical values of the $I2$ center hyperfine (HF) splittings determined in the EPR and ENDOR studies do not agree. The ENDOR spectra presented in Ref. 5 show HF splittings of $A_{\|c}=12.1$ MHz and $A_{\perp c}=6.4$ MHz for the $I2$ center, which correspond to 4.3- and 2.3-G splittings. However the HF splitting measured[1] by 9-GHz EPR for $B\perp c$ is 3.1 G. The HF interactions constants $a=(A_{\|}+2A_{\perp})/3$ and $b=(A_{\|}-A_{\perp})/3$ deduced from these values ($a=8.3$ MHz, $b=1.9$ MHz) do not correspond to those given in the same paper ($a=8.7$ MHz, $b=4.2$ MHz).

We report in this paper new EPR results on the high- and low-temperature spectra of the P related centers. They show

TABLE I. g factors and hyperfine splitting constants A of the shallow and deep phosphorous centers as reported in Refs. 1, 4, and 5.

Center	High T (77 K)		Center	Low T (4.2 K)		Refs.
$P1$	$g\parallel=2.0040$	$A\parallel=56.3$ G				EPR, Ref. 3
	$g\perp=2.0029$	$A\perp=55.5$ G				
$P2$	$g\parallel=2.0040$	$A\parallel=51.7$ G				
	$g\perp=2.0025$	$A\perp=51.7$ G				
P-V	$g\parallel=2.0044$	$A\parallel=9.2$ G				
	$g\perp=2.0025$	$A\perp=7.2$ G				
			$I1$	$g\parallel=2.0049$	$A\parallel=1.2$ G	EPR, Ref. 4
				$g\perp=2.0031$	$A\perp=\leqslant 1.2$ G	
			$I2$	$g\parallel=2.0041$	$A\parallel=6.11$ G	
				$g\perp=2.0028$	$A\perp=1.58$ G	
			$I1$		$A\parallel=1.2$ G	ENDOR, Ref. 5
					$A\perp=0.2$ G	
			$I2$		$A\parallel=4.3$ G	
					$A\perp=2.3$ G	
			$I2$	$g\parallel=2.0041$	$A\parallel=6.1$ G	EPR, Ref. 1
				$g\perp=2.0028$	$A\perp=3.1$ G	

the presence of two different defects in three configurations corresponding to the three nonequivalent lattice sites in the 6H polytype. Our results settle also the question of the localized or delocalized character of the low-temperature defects $I1$, $I2$ by the observation of a superhyperfine (SHF) interaction with two equivalent Si atoms. Further, we show that the so-called high-temperature spectra can also be observed at 4.2 K, which proves that they do not correspond to an excited state of the shallow effective-mass-(EM) like P donor.

EXPERIMENTAL DETAILS

The 6H-SiC:N bulk samples of 400 μm thickness were prepared by the Lely method under special conditions to reduce the N concentration to the 1.2×10^{16}-cm^{-3} level They were irradiated with thermal neutrons to a total dose of 1×10^{20} cm^{-2}.

Thermal neutrons will transmute ^{30}Si isotopes into ^{31}P according to the reaction

$$^{30}\mathrm{Si}+n\rightarrow{}^{31}\mathrm{P}+\beta^{-}.$$

The P concentration thus obtained is estimated to 1.2×10^{16} cm^{-3}. After the irradiation a thermal annealing at 1900 °C for 30 min was performed.

The EPR measurements were performed with a X-band spectrometer. The spectra were measured over the whole temperature range of 4 to 100 K. The g values were determined from the measured microwave frequencies and the magnetic-field values calibrated by a proton nuclear magnetic resonance sonde. To further minimize errors in the field determination, an additional g-standard (MgO:Mn) was used. The error in g is estimated to be $\Delta g<0.0002$. The experimental EPR spectra were decomposed into their individual components with the help of a special computer program, which allowed the determination of line shape, linewidths, line intensities, and positions.

RESULTS

Shallow P donors

Figure 1 shows a typical EPR spectrum observed at $T=80$ K for the magnetic-field orientation $B\parallel c$. In the central part we observe a strong three-line spectrum which originates from the N doping; it is the sum of the three N shallow donor spectra for the $c1$, $c2$, h sites, which are not resolved under these conditions. In addition, we observe three anisotropic doublet spectra named sP_{c1}, sP_{c2}, sP_h, the parameters of which are given in Table II. They are of axial sym-

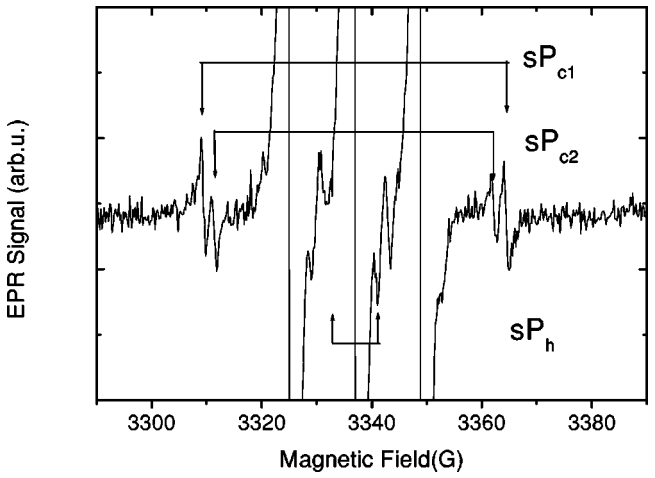

FIG. 1. EPR spectra of the shallow P centers (sP_{c1},sP_{c2},sP_h) at 80 K; $B\parallel c$.

TABLE II. EPR parameters (g factors and phosphorous hyperfine interaction constants A) and thermal ionization energies E of the shallow phosphorous centers.

Center	Model	Center	Model	Energy (meV)
$P1$	$P_{Si}(c1)$	sP_{c1}	$P_{Si}(c1)$	110
$g\|\|=2.0040$		$g\|\|=2.0038$		
$g\perp=2.0029$		$g\perp=2.0028$		
$A\|\|=56.3$ G		$A\|\|=55.0$ G		
$A\perp=55.5$ G		$A\perp=54.2$ G		
$P2$	$P_{Si}(c2)$	sP_{c2}	$P_{Si}(c2)$	110
$g\|\|=2.0040$		$g\|\|=2.0038$		
$g\perp=2.0025$		$g\perp=2.0025$		
$A\|\|=51.7$ G		$A\|\|=51.0$ G		
$A\perp=51.7$ G		$A\perp=51.0$ G		
P-V	P-X	sP_h	$P_{Si}(h)$	80
$g\|\|=2.0044$		$g\|\|=2.0041$		
$g\perp=2.0025$		$g\perp=2.0022$		
$A\|\|=9.2$ G		$A\|\|=9.0$ G		
$A\perp=7.2$ G		$A\perp=7.2$ G		
Veinger *et al.* (Ref. 3)		This work		Troffer *et al.* (Ref. 6)

metry and correspond to the three phosphorous centers previously reported by Veinger *et al.*[3] The g values and HF constants differ slightly from those reported in Ref. 3 probably due to a better field/frequency calibration in our study. We attribute these spectra in agreement with recent calculations by Gali *et al.*[9] to the ground state of the isolated P centers on the three nonequivalent Si lattice sites. The isotropy of the central HF interactions and the weak localization of the wave function are very similar to the case of the shallow N donors and correspond to the properties of an effective mass donor. In spite of the different lattice sites of the N_C and P_{Si} donors, the hexagonal site P_{Si} donor has equally a strongly reduced central HF interaction as compared to the $c1$, $c2$ site donors.

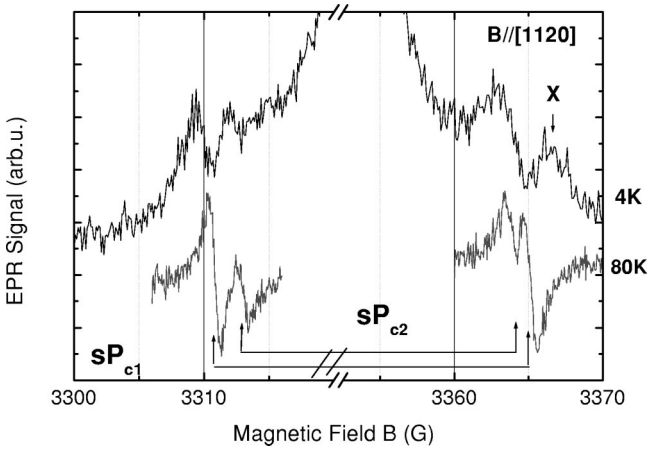

FIG. 2. EPR spectra of the sP_{c1}, sP_{c2} centers at 80 and 4 K for $B\|[1120]$; note an x axis break between 3320 and 3350 G; the high-field X line belongs to a different spectrum.

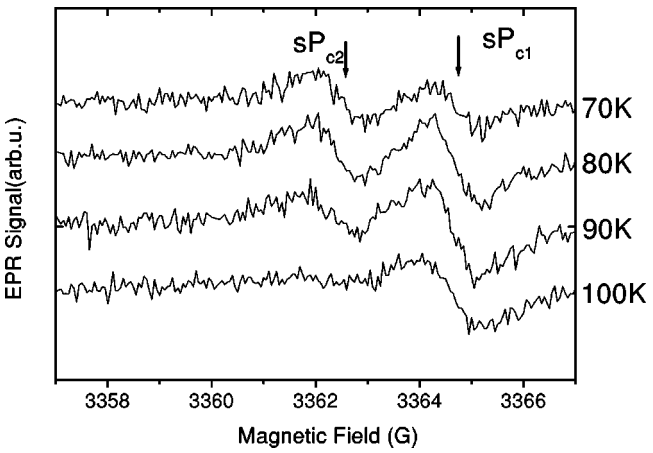

FIG. 3. High-field EPR lines of the sP_{c1}, sP_{c2} centers in the 70–100 K range.

To investigate the issue of the ground- or excited-state configurations, we have measured the temperature dependence of the sP_{c1}, sP_{c2}, sP_h spectra between 100 and 4.2 K. Below 60 K the sP centers saturate even for the lowest available microwave powers of 0.1 μW and their observation under slow passage conditions is no longer possible. However, as shown in Fig. 2, the sP_{c1} sP_{c2} centers can still be observed at $T=4.2$ K under fast passage conditions leading to an absorption line shape. The central part containing sP_h is obscured by the strong N spectrum. As the energy separation between the ground state of the effective mass donor and its first excited state is estimated to be 36 meV for the quasicubic site donors,[1] the EPR observation of the excited donor state is not expected under thermal equilibrium conditions at 4 K due to its negligable thermal population. We can thus attribute the sP_{c1}, sP_{c2} spectra to the ground-state configuration of the phosphorous donor.

The study of the EPR spectra of the sP_{c1}, sP_{c2} centers at high (>80 K) temperatures allows also to determine which of the two quasicubic centers has the smaller thermal ionization energy. In Fig. 3 we show the high field lines of the two spectra at 70, 80, 90, and 100 K. The spectra are taken under

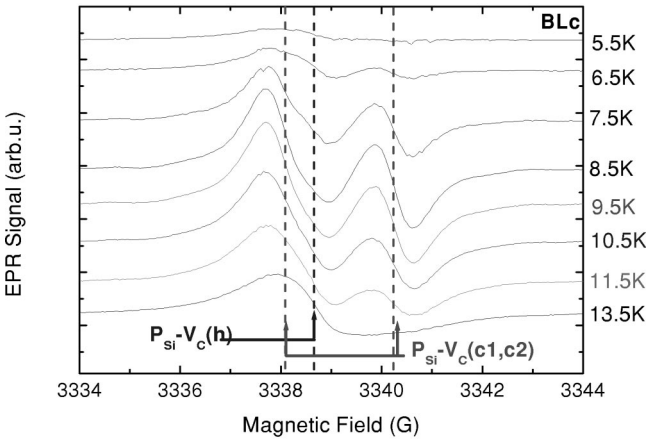

FIG. 4. Temperature dependence of the total deep phosphorous related EPR spectrum.

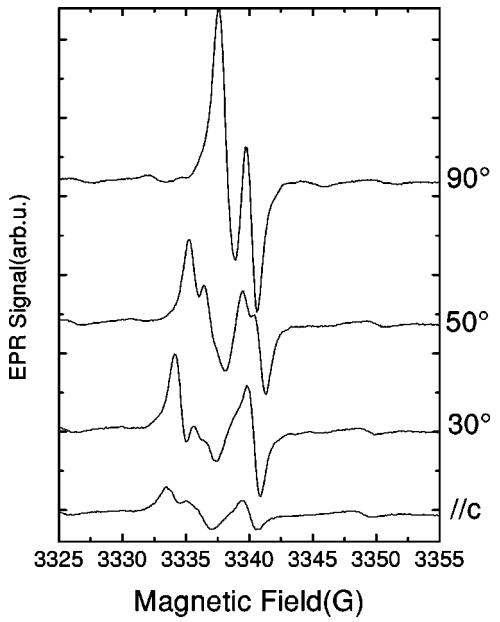

FIG. 5. Low-temperature EPR spectra of the superposed three deep P centers for different field orientations; $T=9$ K.

the same conditions. We observe a slight reduction in the HF splitting of the sP_{c2} center in the 70–90 K range and its disappearance due to thermal ionization at 100 K. Thus, as in the case of N donor, the P donor with the smaller HF interaction corresponds to that with the smaller thermal ionization energy.

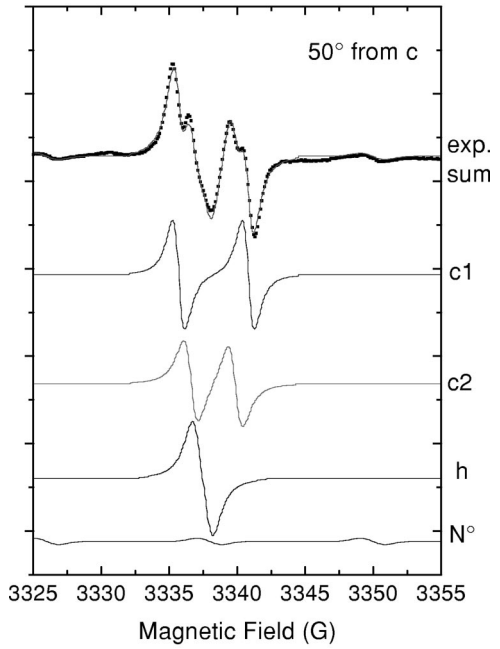

FIG. 6. Decomposition of the experimental EPR spectrum at $T=9$ K and B at 50° from the c axis in four components: three doublet lines corresponding to the deep phosphorous centers on the $c1$, $c2$, h sites and the N spectrum; the sum spectrum (line) is superposed on the experimental one (dots).

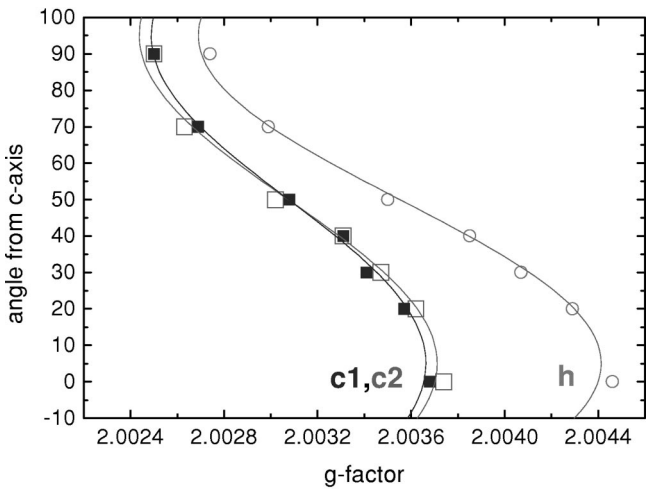

FIG. 7. Angular variation of the g factors of the centers dP_{c1} (squares), dP_{c2} (open squares), dP_h (circles) at $T=9$ K.

Deep P donors

In the 4–15 K temperature range, additional phosphorous related EPR spectra are observed. Figure 4 shows a series of spectra taken under identical conditions for $B\perp c$ between 13.5 and 5.5 K. At the highest temperature, we observe a single line spectrum of axial symmetry; at slightly lower temperatures (11.5 K) an apparent doublet spectrum becomes superimposed. Both can be well studied simultaneously in the 7.5–10 K temperature range. For lower temperatures, all spectra decrease in intensity, and at 4.2 K they are no longer observable. As will be shown below, the total EPR spectrum can be consistently simulated as the sum of three anisotropic doublet spectra, which we label dP_{c1}, dP_{c2}, dP_h; the three spectra show an angular-dependent and temperature-dependent intensity variation typical for Jahn-Teller distorted low-symmetry defects[10] with a thermally activated motional averaging giving rise to an apparent C_{3v} symmetry. The particularity of the system is the unusually low thermal activation energy.

In Fig. 5 typical EPR spectra for different magnetic-field

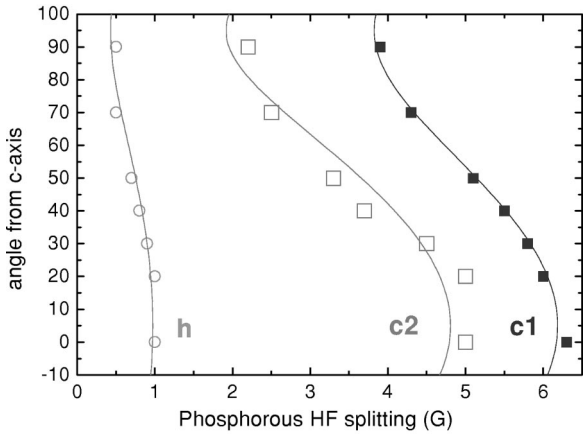

FIG. 8. Angular variation and fit of the hyperfine splitting constant for the dP_{c1} (squares), dP_{c2} (open squares), dP_h (circles) centers.

TABLE III. EPR parameters and microscopic models of the deep phosphorous centers.

Center		Center	Model
$I1$	$I1$	dP_h	$P_{Si}(h)$-V_C
$g\|\|=2.0049$		$g\|\|=2.0044$	
$g\perp=2.0031$		$g\perp=2.0027$	
$A\|\|=1.2$ G		$A\|\|(P)=1.0$ G	
$A\perp=\leqslant 1.2$ G		$A\perp(P)=0.5$ G	
		$A_{SHP}(Si)=11.2$ G	
$I2$	$I2$	dP_{c1}	$P_{Si}(c1)$-V_C
$g\|\|=2.0041$		$g\|\|=2.0037$	
$g\perp=2.0028$		$g\perp=2.0025$	
$A\|\|=6.11$ G	$A\|\|=6.1$ G	$A\|\|(P)=6.2$ G	
$A\perp=1.58$ G	$A\perp=3.1$ G	$A\perp(P)=3.8$ G	
		$A_{SFH}(Si)=8.8$ G	
		dP_{c2}	$P_{Si}(c2)$-V_C
		$g\|\|=2.0037$	
		$g\perp=2.0024$	
		$A\|\|(P)=4.8$ G	
		$A\perp(P)=1.9$ G	
		$A_{SHF}(Si)=10.2$	
4.2 K/142 GHz (Ref. 4)	4.2 K/9 GHz (Ref. 1)	This work 9 K/9 GHz	

orientations are shown. For the two high-symmetry orientations—$B\|c$ and $B\perp c$—the spectra can and have in the past been mistaken as a sum of two doublet spectra only. We performed a detailed computer assisted analysis of the total

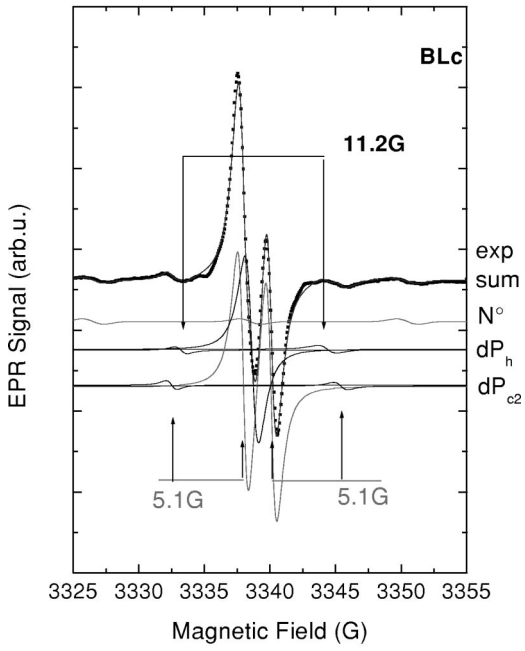

FIG. 9. Experimental EPR spectrum and its decomposition in dP_{c2} and dP_h components with their corresponding superhyperfine lines; $B\perp c$, $T=9$ K; the experimental spectrum (dots) and the sum spectrum (line) are superposed.

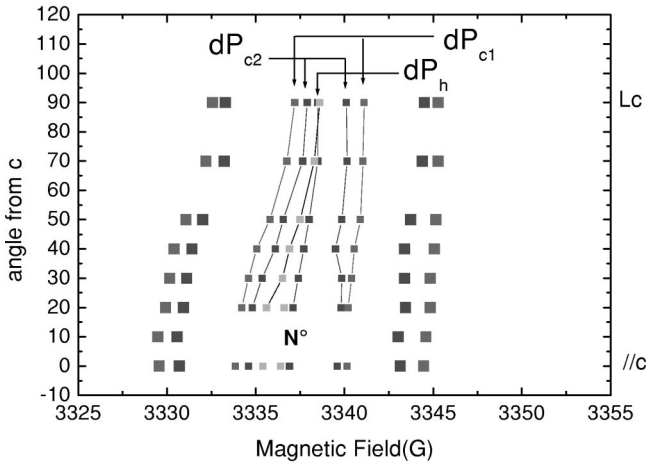

FIG. 10. Angular variation of the SHF lines (large squares) of the deep P centers; for $B\perp c$ the intensity of the dP_{c1} center is small as compared to the other two centers and a good assignement is possible. For the other orientations the superposition of the SHF lines from the three centers will require high-frequency studies for the determination of the small anisotriopy of the SHF tensors.

EPR spectrum for all magnetic-field orientations. They show clearly the presence of three partially overlapping doublet spectra and not two, as previously assumed. The presence of three spectra is most easily seen at intermediate angles where all three are of comparable intensities. The decomposition for the orientation 50° from c is shown in Fig. 6. The contribution of the underlying N spectrum, small under these experimental conditions, is included in the decomposition. The complete analysis of the angular variation shows the presence of three spin $S=\frac{1}{2}$ spectra with axial symmetry for the g tensor and the central phosphorous hyperfine interaction. The effective g factors and hyperfine splittings are represented in Figs. 7 and 8. The principal values obtained by a least-squares fit are given in Table III.

The variation of the intensity of the spectra with the magnetic-field orientation is particularly important for the spectra of deep P centers dP_{c1} and dP_{c2}. As a consequence for $B\|c$, the dP_{c1} doublet is dominating whereas for $B\perp c$ the dP_{c2} doublet is strongest. As the g values of the two centers are very close this can easily give rise to a misinterpretation of the experimental result.

The dP spectra show additional small intensity lines due to superhyperfine (SHF) interaction; they can easily be seen for $B\perp c$ at the low- and high-field sides of the central set of lines (Fig. 9). For this orientation, where the $dPc2$ and dPh spectra are dominant in intensity, we observe two doublets centered at the dP_{c2} and dP_h lines, respectively, with splittings of 10.2 G (dP_{c2}) and 11.2 G (dP_h). For $B\|c$ a value of 8.8 G is obtained for dP_{c1}. The intensity ratio of the SHF lines to the corresponding central line has been evaluated to 10%, which corresponds to the interaction with two equivalent Si atoms (Table III). The SHF structure is observable for all orientations; it is approximately isotropic with values in the 10-G range (Fig. 10). A more refined analysis of its small angular dependence requires the use of higher microwave frequencies.

DISCUSSION

The simultaneous observation of three shallow and three deep phosphorous related centers allows a coherent interpretation of the shallow phosphorous defects within the EM model. Whereas for the $P1$, $P2$ centers, the attribution to substitutional P on silicon $c1$, $c2$ sites was accepted since long, their ground state (A_1/E) and the attribution of the third so-called P-V center remained controversial.[1,5,8] From our results it follows that the shallow P donor ground state is an A_1 state, and thus the three EM-like P centers should have spin densities at the P nuclei in close analogy to the nitrogen EM-like donors. This corresponds to the experimental findings: the isotropic HF interaction constants scaled with the nuclear g factors (a/g_N) are 82.28/83.13/6.11 MHz for the N donors at the $c1$, $c2$, h sites, and 64.09/68.93/9.7 MHz for the corresponding P donors. (The value of 1.06 MHz given in Ref. 1 is erroneous. It is more correct to take into consideration the *s*-electron wave function density at N and P nucleus for nitrogen and phosphorous atoms that corresponds to[11] 5.599 a.u. and 7.252 a.u., respectively, and overlap integrals between envelope function and wave functions of N and P. But for a qualitative analysis we will not consider these effects because they partly compensate one another.) As the $P1$, $P2$, P-V EPR spectra had not been observed at low temperature in the previous studies the possibility of a thermally populated excited A_1 state and thus an E ground-state configuration had been considered.[1] However, our observation of the quasicubic shallow P centers at 4.2 K exclude this possibility and show a complete analogy between the shallow N and P donors in 6H-SiC in spite of their different lattice sites C/Si. Our assignment is in good agreement with recent calculations by Gali *et al.*,[9] who predicted also the A_1 character of the EM-like P donor ground state.

The observation of strong SHF interaction with two Si neighboring atoms demonstrates the deep character of the second set of phosphorous defects (*dP*) observed at low temperature. The reduced HF interaction with the P nuclei as compared to the EM donors seems at first surprising, as with a more localized wave function, a higher P HF interaction might have been expected. Recent calculations[9] of the spin distribution of the P-vacancy complex, which is a highly probable candidate for the *dP* centers, are however in good agreement with our experimental results. Gali *et al.*[9] have modeled the neutral P_{Si}-V_C center in 3C geometry using a $C_{37}Si_{34}H_{60}$ molecular cluster. Their results show that the paramagnetic electron is not localized on the P atom but on a Si atom in the first nearest-neighbor position of the carbon vacancy. The ground state corresponds to one electron occupation of an *e*-level subject to a Jahn-Teller distortion $C_{3v} \rightarrow C_{1h}$. Their calculations confirm the localized character of the ground-state wave function: in the C_{1h} symmetry relaxed state 85% of the spin density is localized within the first and second neighbor shells; the main spin density is not on the P atom but on the three next-nearest-neighbor Si atoms of the carbon vacancy with 44.2% on (Si_1) and 9.6% on (Si_2,Si_3). The localization on the P atom is only 2.1%. Due to the strong localization of the wave function these results are also considered to be relevant for the 6H polytype. The predicted P and Si SHF interaction are in qualitative agreement with the experimental results obtained for the three deep P centers. The additionally predicted strong HF interaction with one Si_1 atom has not yet been observed up to now. Nevertheless, we consider these results to be a strong support for the assignment of the deep P centers to the P_{Si}-V_C pairs on the three $c1$, $c2$, h lattice sites.

TABLE IV. Comparison of the EPR parameters (g factors, hyperfine and superhyperfine interaction constants A) of the N_C-V_{Si} and the dP_h (P_{Si}-V_C) pairs

N_C-V_{Si} pair	Si-V_C pair/hexagonal site
$S=\frac{1}{2}$ C_{3v}	$S=\frac{1}{2}$ C_{3v}
$g\parallel=2.0063$	$g\parallel=2.0044$
$g\perp=2.0044$	$g\perp=2.0027$
$A\parallel$(N)$=1.0$ G	$A\parallel$(P)$=1.0$ G
$A\perp$(N)$=0.8$ G	$A\perp$(P)$=0.5$ G
$A\parallel$(3C)$=15.0$ G	A_{SHF}(2Si)$=11.2$ G
$A\perp$(3C)$=10.5$ G	
Vainer *et al.* (Ref. 12)	This work

It is instructive to compare the properties of the deep P centers with the deep N center[12] observed in fast neutron irradiated, thermally annealed *n*-type 6H-SiC:N and the deep B and deep Al centers[13] observed often as native defects. Under fast neutron irradiation conditions ^{31}P generation by transmutation is negligible and only intrinsic point defects and defect complexes are generated by elastic collisions. During high-temperature annealing, the point defects become mobile and can interact with the dopant atoms—N in this case. Vainer and II'in[12] have reported after annealing in the 1350–1950 °C range the formation of a new nitrogen related defect characterized by a strongly reduced N HF interaction and resolved C SHF interaction. This center has been attributed to a N_C-V_{Si} pair. A comparison with the corresponding P centers shows (Table IV) a close similarity with the hexagonal site deep phosphorus center dP_h. This analogy further supports the attribution of the deep phosphorous centers to P_{Si}-V_C pairs. It might appear astonishing that in our samples only defects of C_{3v} symmetry are observed whereas one should expect also the occurrence of P_{Si}-V_C pairs not aligned with the c axis. However, different explanations can be considered for their nonobservation: e.g., the thermal stability of such complexes might be different; it must be recalled that the samples of this study were annealed at 1900 °C, the electrical levels of deep defects in SiC vary with the local symmetry and their observation depends on particular Fermi-level positions which might not be favorable in our samples.

As concerns the angular- and temperature-dependent intensity variation observed for the deep P centers it should be noted that a similar behavior has previously been reported for the deep B and deep Al centers, which were also suggested[13] to be carbon vacancy complexes.

The microscopic nature of the defects remaining after very high ($T>1500$ °C) temperature thermal annealing has been the object of numerous studies but no conclusion could be drawn. The $D1$ defect (see Refs. 14 and 15 and references

therein) easily observable in photoluminescence is the principal defect observed after such treatments. The EPR results on the neutron irradiated and 1900 °C annealed samples add new elements to this discussion: they demonstrate a surprising and unexpected formation and thermal stability of donor—monovacancy complexes; this contrasts sharply with the weak thermal stability of the isolated monovacancies, which anneal out below 1000 °C. Veinger *et al.*[3] had observed that the concentration of the shallow phosphorous centers decreases after the annealing at high temperature. We believe that the formation of the deep P center is a result of the capture by the shallow P center of the carbon vacancy, which is released in this high-temperature annealing step. In agreement with this correlation the involvement of vacancies in high-temperature defects including the $D1$ center can be concluded. The involvement of the Si vacancy in the $D1$ center has recently been proposed by Fissel *et al.*[16] from photoluminescence studies on growth related $D1$ defects.

CONCLUSION

We have shown that phosphorous donors introduced by neutron transmutation give rise to both shallow and deep phosphorous centers in close analogy to the case of the nitrogen dopant. For both *sP, dP* defects, the three-site specific centers have been observed and characterized. The deep phosphorous center is attributed to a P_{Si}-V_C complex formed in the high-temperature annealing step.

ACKNOWLEDGMENTS

We thank the CNRS-DRI (Contract No. 7780) for partial financial support of this work. P.G.B, I.V.I., and E.N.M. thank RFBR (Grant No. 00-02-16950) for partial support of this work.

[1] S. Greulich-Weber, Phys. Status Solidi A **162**, 95 (1997); S. Greulich-Weber, Phys. Status Solidi B **210**, 415 (1998).
[2] A. v. Duijn-Arnold, R. Zondervan, J. Schmidt, P. G. Baranov, and E. N. Mokhov, Phys. Rev. B **64**, 085206 (2001).
[3] A. I. Veinger, A. G. Zabrodskii, G. A. Lomakina, and E. N. Mokhov, Fiz. Tverd. Tela **28**, 1659 (1984) [Sov. Phys. Solid State **28**, 917 (1986)].
[4] E. N. Kalabukhova, S. N. Lukin, and E. N. Mokhov, Fiz. Tverd. Tela **35**, 703 (1993) [Phys. Solid State **35**, 361 (1993)].
[5] S. Greulich-Weber, M. Feege, J-M. Spaeth, E. N. Kalabukhova, S. N. Lukin, and E. N. Mokhov, Solid State Commun. **93**, 393 (1995).
[6] T. Troffer, C. Peppermuller, G. Pensl, K. Rottner, and A. Schoner, J. Appl. Phys. **80**, 3739 (1996).
[7] H. Heissenstein and R. Helbig, Mater. Sci. Forum **353–356**, 369 (2001).
[8] S. Greulich-Weber, Phys. Status Solidi B **210**, 415 (1998).
[9] A. Gali, P. Deak, P. R. Briddon, R. P. Devaty, W. J. Choyke, Phys. Rev. B **61**, 12 602 (2000).
[10] W. E. Carlos, E. R. Glaser, and D. C. Look, Physica B **308–310**, 976 (2001).
[11] J. R. Morton and K. F. Preston, J. Magn. Reson. **30**, 577 (1978).
[12] V. S. Vainer and V. A. II'in, Fiz. Tverd. Tela **23**, 2449 (1981) [Sov. Phys. Solid State **23**, 1432 (1981)].
[13] P. G. Baranov, I. V. Ilyin, and E. N. Mokhov, Solid State Commun. **100**, 371 (1996).
[14] T. Dalibor, G. Pensl, T. Kimoto, H. Matsunami, S. Srindhara, R. P. Devaty, and W. J. Choyke, Diamond Relat. Mater. **6**, 1333 (1997).
[15] T. Egilsson, J. P. Bergman, I. G. Ivanov, A. Henry, and E. Janzen, Phys. Rev. B **59**, 1956 (1999).
[16] A. Fissel, W. Richter, J. Furthmuller, and F. Bechstedt, Appl. Phys. Lett. **78**, 2512 (2001).